

Localized air-conditioning with occupancy control in an open office

L. James Lo, Atila Novoselac*

University of Texas at Austin, 1 University Station C1752, Austin, TX 78712, USA

ARTICLE INFO

Article history:

Received 15 January 2010

Accepted 3 February 2010

Keywords:

Occupancy control
Localized airflow
Zoning
Open office
Contaminant removal
Indoor air quality
HVAC energy
CFD

ABSTRACT

Conditioning and ventilating open office spaces requires innovations as new buildings aim to be more intelligent, energy efficient and healthy. This paper explores the possibility of using a localized airflow to divide an open cubicle office into zones without partition walls. Computational fluid dynamics (CFD) model was used to simulate localized airflow in a cubicle office and both the energy and the indoor air quality concerns were addressed. The findings suggest that (1) localized airflow is plausible for zoning purposes, (2) localized airflow can result in both temperature and pollutant concentration segregations, (3) temperature segregations provide possible energy savings if coupled with occupancy-based HVAC control, and finally (4) limited air mixing between zones provide a novel way for better ventilation and indoor contaminant control.

© 2010 Elsevier B.V. All rights reserved.

1. Introduction

Millions of people spend their workdays in office spaces; in the United States alone, more than 35 million people [1] work in an office environment. Providing adequate ventilation and comfort for these office workers is necessary to maintain a healthy workforce and high productivity [2] for businesses. However, Fisk et al. [3] showed that indoor air quality (IAQ) issues in offices are prevalent. Increasing the ventilation rate can often reduce this IAQ problem [4], but a larger ventilation rate also translates to a significantly higher energy cost. Therefore, the ability to maintain high indoor thermal and air quality conditions while minimizing energy expenses is crucial for an optimized building HVAC system.

One possible solution towards achieving an optimal HVAC system is to couple occupancy control strategies with ventilation and HVAC systems. An occupancy-based ventilation and air-conditioning control system can deliver fresh conditioned air to the indoor spaces only when they are occupied. Occupancy-based control is a well-developed concept already applied in commercial applications. In the 1990s, Fountain et al. [5] indicated this need of using occupancy controls in hotels and other public buildings with short term and variable occupancy. Furthermore, Rabl and Rialhe [6] used energy models to show occupancy-based HVAC control in commercial buildings could lead to significant energy savings.

However, employing occupancy-based controls is difficult in many places, such as an open office, without walls to divide the area into environmental zones. If a thermal and flow isolated space could be created in an open office, then occupancy-based control strategies could also be realized in this setting.

Creating an isolated environment in an open office might be possible via a localized flow by using multiple slot diffusers to provide angled supply jets and a central return vent to limit the spreading-out air movements. The analyzed localized airflow is shown in Fig. 1.

This type of localized airflow creates an indoor environment which is different from typical airflow distribution systems such as standard square or round ceiling diffusers that use Coandă effect to distribute the air in the space. Due to lack of Coandă effect with appropriate direction of the supply jet (Fig. 1), a favorable condition for localized flow and large office zoning is attainable. In some situations this condition could result in an improved energy and ventilation performance if the zoning effect is prominent. To test this hypothesis, airflow and energy analysis were conducted by simulating airflow described in Fig. 1.

This study investigates three different aspects of using localized airflow in an office space. The first aspect determines whether the air supply and exhaust configuration shown in Fig. 1 can produce a stable airflow and thermal conditions for the open-zone occupancy controlled concept. The second aspect extends the airflow analysis specifically on study of ventilation and contaminant removal effectiveness, which defines indoor air quality. The third aspect includes an energy simulation analysis for a typical office building

* Corresponding author. Tel.: +1 512 475 8175.

E-mail address: atila@mail.utexas.edu (A. Novoselac).

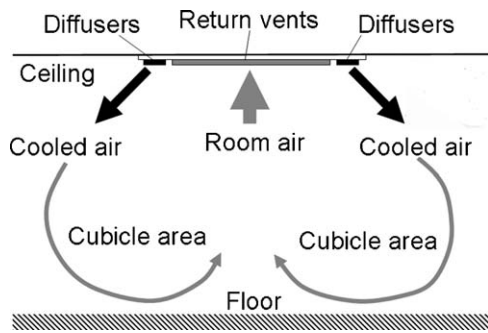


Fig. 1. Diffuser with integrated supply return vent with the characteristic airflow distribution in an occupied zone of an open cubicle office space.

with occupancy-based control and zoning by localized airflow, which determines energy saving potentials.

2. Methods

This study used experimental measurements and computational fluid dynamics (CFD) modeling for airflow and air quality analyses, as well as energy simulations for energy analyses. Details related to the methodologies for each of the three considered aspects are provided in the following sections.

2.1. Airflow modeling

To contain airflow inside a designated zone, typical ceiling diffusers cannot be used as they rely on the *Coandă* effect and would carry conditioned air away from the targeted space. To produce the specific airflow described in Fig. 1, a configuration using a single center return vent surrounded by four thin slot diffusers with outward-angled slots was selected for this study. This configuration was selected because it is similar to typical commercial mini-split HVAC systems currently available on the market.

For this selected configuration, it is crucial for the accuracy of the analysis that the diffuser characteristics, such as jet intensity and direction, are known for the CFD diffuser modeling. To obtain real diffuser characteristics, a full-scale chamber experiment was conducted where airflow parameters were measured for a slot diffuser identical to the size and function of the selected configuration. The diffuser's variable supply adjuster fin was used to mimic the angle of the outward flow from one of the four slots. In this jet validation experiment, a flow rate of $0.047 \text{ m}^3/\text{s}$ was used for a single side supply jet. This number is based on the design flow rate ($0.19 \text{ m}^3/\text{s}$) of a similar commercially available mini-split system unit with four-side diffusers in the same space. Furthermore, the air jet experimented was adiabatic (at room temperature), and the flow field was only affected by the diffuser momentum without effect of buoyancy. The justification of using an adiabatic jet is that the experimental supply jet discharge velocity is large ($>2 \text{ m/s}$) and momentum forces are dominant within the vicinity of the supply diffuser. For the data collection, forty velocity monitor points were measured in a $0.5 \text{ m} \times 1 \text{ m}$ vertical plane along the jet direction, and the experiment was repeated to ensure the accuracy of the results.

Experimental jet characteristic data provided the necessary pieces to construct the CFD model. To create a model that can capture air jet properties measured in the experiments, several methods were considered. Huo et al. [7] proposed a systematic method to simulate a diffuser by describing the complicated boundary conditions in term of surrounding air volumes. Srebric and Chen [8] introduced an even more simplistic way to model the

diffusers, using either the box or the momentum methods, not describing the diffuser behavior directly, but its resulting airflow. Since the primary concern for this study is the resulting airflow within the zone away from the diffuser, the momentum method was selected. Matching the experimental validation, the supply jet was simulated adiabatically as well. Cell sizes of 5 cm and 3 cm were used in CFD simulations to verify grid independency, and RNG $k-\epsilon$ turbulence model [9] was used to assess the effects of small eddies in Reynolds Averaged Navier Stokes Equations. The comparison of experimental data and the CFD model evaluated the accuracy of CFD diffuser geometry, grid resolution and the turbulence model. The detailed validation results are provided in the result section of the paper.

After the adjustment of critical simulation parameters such as the computation mesh and diffuser boundary conditions validated experimentally, the CFD diffuser model were placed in a large space that represents the different cubicle setups of a multi-zone office. For a single zone in a large open office space, a typical office cubicle area in a shape of $2.44 \text{ m} \times 2.44 \text{ m}$ square was selected. The CFD zone model was setup with both heat-flux (office equipment, occupants and reradiating lighting load) and mass-flux (supply jet) boundary conditions. After verifying the grid dependency, a 20 cm grid size was selected for the model resulting in 150,000 cells for a single zone simulation and 300,000 cells for two connected zones. Simulating an airflow in the large room with only diffuser validation might raise some concerns, however the critical CFD parameters such as computation grid resolution and boundary conditions were selected based on authors' previous CFD validation experiments of buoyancy and jet driven airflow in small and large spaces [10,11], showing that CFD can accurately simulate the flow regimes away from the diffuser as well as the effect of the buoyancy forces.

To analyze different airflow scenarios in the cubicle office, a six-cubicle configuration was selected and connected in two different orientations, shown in Fig. 2. In addition to the diffusers and the return vents, this zone model also included 1.5 m high cubicle walls and box representations of internal loads, including occupants, equipments and lighting radiation effects. Recommendations from ASHRAE [12] were used to select proper values for the internal loads: 75 W sensible load for seated occupants, 70 W as a high estimate for continuous computer operation and additional 20 W/m^2 for other internal loads included reradiating and lighting loads.

By connecting two of these zone models together, the airflow between the zones can then be simulated using CFD. Two

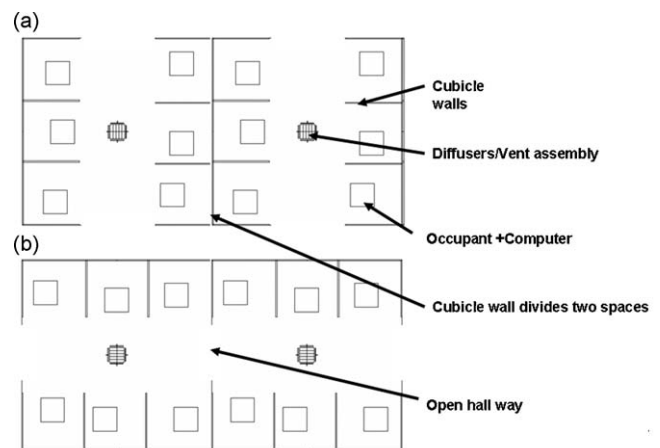


Fig. 2. Two cubicle orientations and components used in the CFD model: (a) back-to-back cubicle setup with half height cubicle wall divide the zones and (b) side-to-side cubicle setup with an open hall way.

Table 1
Parametric analysis of CFD simulations.

Case	Description	Left zone HVAC	Dynamic load (W)
A-1	Cube orientation "a" with full occupancy and equipment operation in both zones	On	870
A-2	Same as A-1 but with left zone at half occupancy and equipment operation	On	435
A-3	Same as A-1 but with left zone unoccupied and equipment turned off	Off	0
A-4	Same as A-3 with an additional load to simulates scenario with larger adjacent unoccupied space	Off	1740
B-1	Cube orientation "b" with full occupancy and equipment operation in both zones	On	870
B-2	Same as B-1 but with left zone at half occupancy and equipment operation	On	435
B-3	Same as B-1 but with left zone unoccupied and equipment turned off	Off	0
B-4	Same as B-3 with an additional load to simulates scenario with larger adjacent unoccupied space	Off	1740

orientations to be modeled in this study: (1) identical unit spaces with the back-to-back cubicle walls and (2) spaces with cubicles side-to-side (Fig. 2). For these two configurations of multi-zone models, parametric analyses were conducted considering the effect of the different cooling loads (dynamic cooling loads vary only due to occupancy changes) and operation scenarios presented in Table 1. The scenario criteria consist of the two cubicle orientations as shown in Fig. 3, whether the HVAC system is in operation and the change in total dynamic internal load. The HVAC on/off parameters illustrate the difference between occupied and unoccupied zones while the four different cooling loads indicate what occupancy included heat source is present for each scenario. For an unoccupied zone, people and computer loads were not present, but the 20 W/m² other heat sources remained to account for non-occupant loads such as release of accumulated heat and lighting.

Some questions can be answered from the CFD simulation results of the scenarios listed in Table 1. Firstly, CFD analysis will show whether the airflow produced in the office space is similar to Fig. 1, given the boundary conditions obtained from the validation experiment. Secondly, the velocity and temperature profiles will determine whether occupant comfort criteria have been met. Thirdly, CFD temperature profiles across the two connected office zones can determine whether a thermal separation is present. And finally, the stability of the localized flow can be determined by increasing side flow such as sudden pressure and flow changes from the surrounding environment.

The CFD airflow analysis in this study is conducted under the assumption of steady state flow conditions in the office space. While some indoor environmental boundary conditions, such as surface temperatures, change slowly, the indoor airflow field establishes a steady flow pattern in a short period of time, often minutes [13]. Since air velocities and temperatures are the only concern in this study, multiple scenarios of steady state simulations were used instead of unsteady state transient simulations. In addition to the steady state assumption, only the cooling scenarios

were considered in this study because: (1) office spaces usually require year-round cooling due to a variety of internal heat sources, and (2) heating scenario would produce a complete different flow regime which is outside of the scope of this study.

While the CFD velocity and temperature results described in this section could demonstrate how effective are the flow patterns and temperature fields created by the localized flow, it could not specifically determine the intensity of inter-zone air mixing. To further investigate the air mixing behaviors between the zones, an age-of-air study was conducted to determine whether the partitioning/curtaining effect is present.

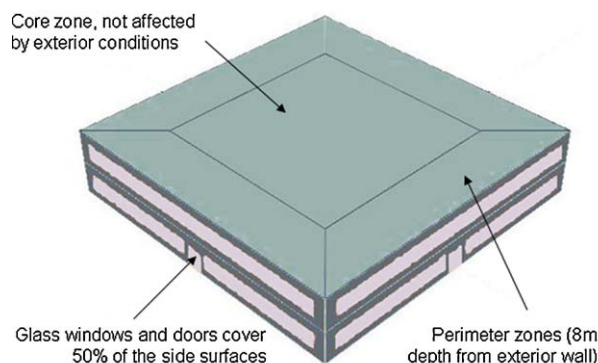
2.2. Air quality modeling

While the air velocity and flow profile are helpful to determine the pollutant transport path, they are ineffective in determining the air mixing nature of the flow and contaminant concentration. By analyzing the effectiveness of air mixing, this study also provides knowledge about the level of air mixing between two zones and assesses occupants' exposures to localized indoor contaminants.

To investigate the level of air mixing between the two zones shown in Fig. 1, the distribution of the age of air in the space, which can be interpreted as the air distribution pattern in the space, were analyzed. Using the physical model and the operation scenario from Fig. 1, a CFD model was adjusted for analysis of the ventilation effectiveness. Eq. (1) shows a direct relationship of the age of air (τ) and ventilation effectiveness as detailed in descriptions by Sandberg [14]:

$$E_v = \frac{\tau_n}{\langle \tau \rangle} \quad (1)$$

To determine the effects of localized airflow on human exposure to common indoor gaseous pollutants, the distribution of formaldehyde (CH₂O) is analyzed. Formaldehyde was selected due to its connections to sick building syndrome [15]. The source of formaldehyde was modeled for three different source locations



Size	2 story, 2300 m ² office
Construction	2x4 metal frame construction with CMU exterior, built up roof
Insulation	Typical R-19 batt insulation
internal partitions	air, to simulate open office
Total HVAC zones	10, 5 per floor (1 core, 4 perimeter)
HVAC system	Packaged DX per zone, to simulate occupancy controlled system
Internal Loads	Same as CFD study
Location	Austin, TX
Simulate Period	TMY2 June, July and August

Fig. 3. Model of the simulated office building in DOE2.2 energy simulation software.

Table 2
Parametric analysis of energy simulations.

Case	Description	Occupancy		Set point	
		Core	Perimeter	Core	Perimeter
1 Base	Full occupancy in both core and perimeter zones	Yes	Yes	24 °C	24 °C
2 NC24	Unoccupied core zones with no temperature set point adjustments	No	Yes	24 °C	24 °C
3 NC29	Unoccupied core zones with temperature set point adjustments	No	Yes	29 °C	24 °C
4 NP24	Unoccupied perimeter zones with no temperature set point adjustments	Yes	No	24 °C	24 °C
5 NP29	Unoccupied perimeter zones with temperature set point adjustments	Yes	No	24 °C	29 °C

from (1) walls, (2) floor, and (3) a point source in the middle of the occupied zone. By selecting these three types of source positions, this simulates common contaminant release scenarios such as new carpets and pressed wood furniture as well as composite materials in the cubicle walls. The effect of airflow on pollutant concentration was analyzed using the contaminant removal effectiveness (ε), which is a ratio of the pollutant concentration at the exhaust (C_e) and the local concentration, detailed by Etheridge and Sandberg [16]:

$$\varepsilon = \frac{C_e}{\langle C \rangle} \quad (2)$$

While formaldehyde was chosen as the emission source, the dimensionless (ε) is a function of the airflow field; it can be applied to indoor pollutants other than formaldehyde as long as the emission source is gaseous and follows similar transport paths. This is useful especially in a point source situation, where the source could be an intentional or accidental release of a certain chemical or an airborne virus originated from an occupant.

Contaminant confinement behavior was also investigated by modeling an emitting source of contaminant inside a cubicle at the breathing plane in two occupied zones (instead of the single occupied zone described previously). This illustrates a scenario where a sick worker in the cubicle and the contaminant removal effectiveness shows how effective the airflow can contain the spread of possible diseases. While it is understood that the virus and bacteria are carried on aqueous particles, a gaseous emission source was used for this simulation. Murakami et al. [17] illustrated that gaseous estimation can be a good indicator for very small ($<1 \mu\text{m}$) particles transport. Additionally, since the larger particle would likely settle earlier and faster than the small ones, the gaseous simulation will overestimate the transport of larger particles, resulting in a worse-case scenario. Therefore, the contaminant effectiveness found using gaseous representation should still be a valid and conservative estimation.

2.3. Energy modeling

To effectively determine whether this localized airflow zoning can provide any benefit regarding to building energy consumption, scenarios based on occupancy control must be considered. However, it is difficult to generate a “typical” occupancy scenario to simulate all buildings as the operations of buildings vary significantly with different users. The particular cases used in this study considered only the scenarios where partial occupancy was prominent and several areas of the building were empty. New and remodeled office buildings are often divided into core and perimeter zones, and this study used either the perimeter or core zones as occupied/unoccupied area of the building. This division could provide results that determine whether energy savings are obtainable and define in which part of the building the occupancy-based control strategy has larger impact on energy usage.

For the energy simulation process, DOE2.2 software package was selected [18]. This allowed us to parameterize the occupancy

and equipment operation schedule, and assign HVAC zones and equipment efficiently. The building being simulated is shown in Fig. 3 as well as the major assumptions used for the energy model.

Once the building energy model was generated, two variable perimeters, occupancy profile and temperature set point, were used for the parametric analysis. A total of six occupancy scenarios were simulated based on these parameters, shown in Table 2.

The occupancy parameters in Table 2 determine how effective the use of occupancy control would be for either core or perimeter zone defined in Fig. 3. The set point parameter determines how HVAC temperature set point would affect the energy use when combined with occupancy control. The occupied set point of 24 °C used here is the design temperature selected for the occupied zone, while the unoccupied set point of 29 °C is used based on calculation of the average free floating temperature inside the building for the geographical location selected (Austin, TX).

The analysis of parameters, defined in Table 2, answers the two questions involving occupancy-based control: (1) Can the strategy of using occupancy control to adjust temperature set point save energy? and (2) Where are the optimal zones to deploy this strategy in a building?

Because the localized airflow investigated in this study is valid only for cooling (air-conditioning with no heating), the three summer months (June, July and August) were selected as these months have no requirements for heating. This specific case, with the three hottest months in a hot climate, represents the best-case scenario for energy saving, determining the potential of the occupancy-based localized airflow control strategy.

3. Results and discussions

The following section details the simulation results obtained from three different investigations described in the methods section. First, the airflow CFD investigation provides jet validation, zonal velocity and temperature profiles, answering the question of whether the localized airflow zoning is possible. Secondly, further CFD contaminant analysis provides results of localized airflow's impact on indoor air quality. Finally, the DOE2 energy analysis provides estimated HVAC energy usage when localized airflow coupled with occupancy control, answering the questions of whether any energy benefit is possible.

3.1. Experimental validation of CFD supply jet model

The result of the validation experiment and CFD simulation is presented in Fig. 4, which shows the comparison of velocity results between experiment and CFD simulation at seven different points, labeled on the jet profile diagram. The results show that, with our selected geometry, turbulence model and grid resolution, the CFD simulation provided very similar diffuser airflow compared to the experiments. The difference in measured and calculated velocity intensity is within the instrumentation uncertainty. Therefore, it is believed that the specific diffuser jet behavior was simulated realistically and can be used for the larger zone based study.

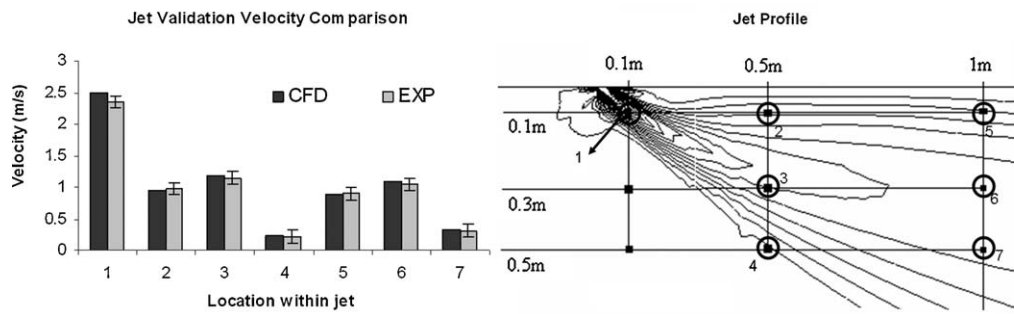


Fig. 4. Validation of CFD diffuser modeling: velocity comparisons and jet profile.

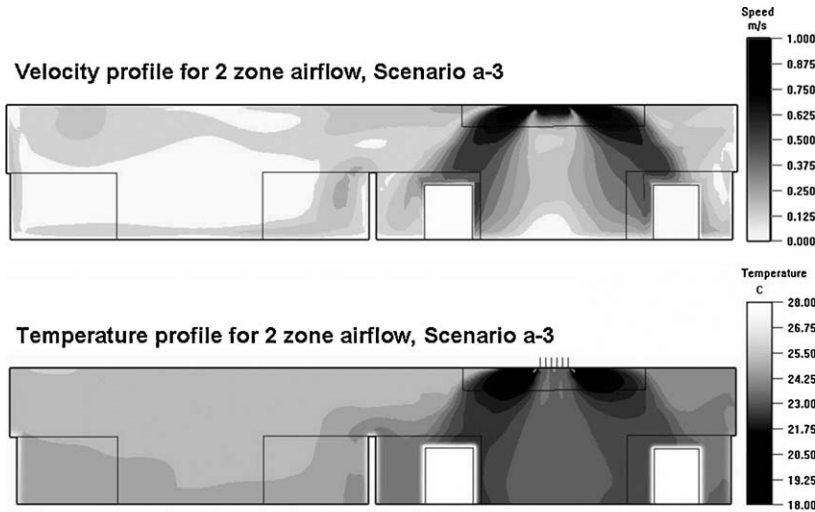


Fig. 5. Velocity and temperature distribution for two adjacent occupied and unoccupied zones (Scenario A-3 from Table 1).

3.2. Airflow simulation

The results in this section show the airflow and temperature distribution, as well as the characteristic parameters such as air mixing intensity and thermal comfort within the zones. Airflow and temperature distributions are presented for one representative scenario in Fig. 5, while thermal comfort and temperature gradient parameters in zones are summarized for all scenarios in Fig. 6.

Fig. 5 illustrates the flow pattern and resulting temperature gradient between the two identical adjacent zones when the right side zone is occupied (with air-conditioning on) and left side zone is unoccupied (with air-conditioning off). Both the shape of the flow (velocity profile) and the horizontal temperature gradient across the zones are evident. The “curtain” effect generated from

the diffusers is slightly different from the shape obtained in the validation (Fig. 2) due to the inclusion of the energy model (no longer adiabatic) to account for buoyancy. Fig. 5 shows that the throw of the jet drops towards the occupancy zone as colder conditioned air sinks down. Therefore, Fig. 5 confirms that the airflow illustrated in Fig. 1 is possible, that the curtain jets along with the zonal return vent can generate a zoning localized airflow within the conditioned space. This phenomenon remains true throughout all eight parametric scenarios (Table 1). Further analysis of these parametric scenarios is presented in Fig. 6.

Fig. 6a shows the averaged air velocity in the vicinity of an occupant’s head. These velocities are between 0.15 and 0.2 m/s, which are within the comfort zone limits established in ASHRAE Standard 55 [10] (less than 0.25 m/s). This demonstrates that the supply jets and airflow distribution in this case are not too “breezy”

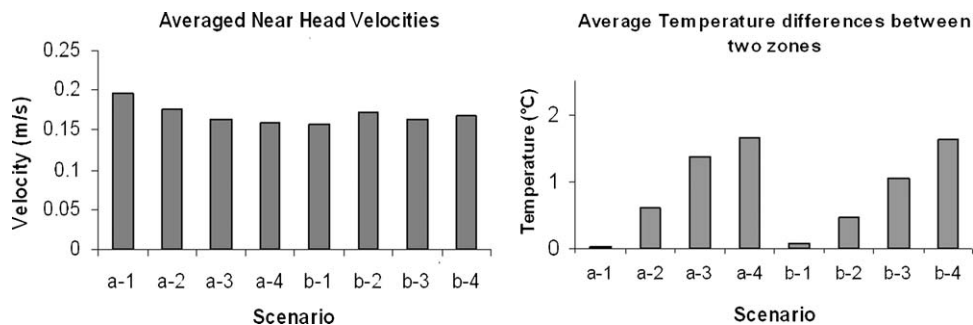


Fig. 6. Impact of localized airflow on thermal comfort parameters and space partitioning: (a) near head velocity and (b) temperature differences between the two zones (scenarios are described in Table 1).

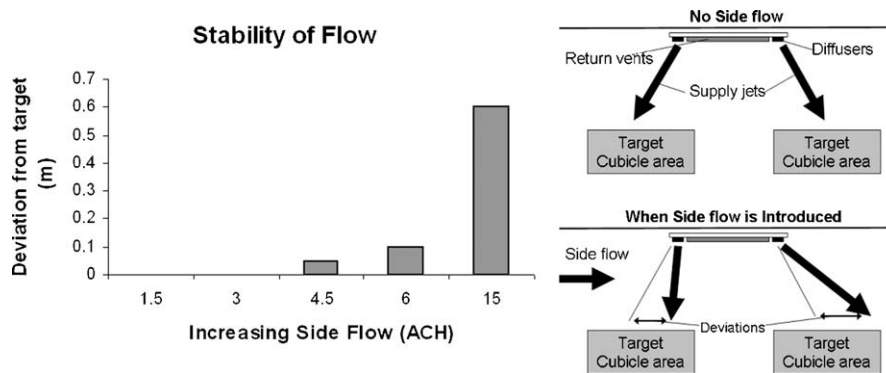


Fig. 7. Stability of the localized flow when side flow is introduced.

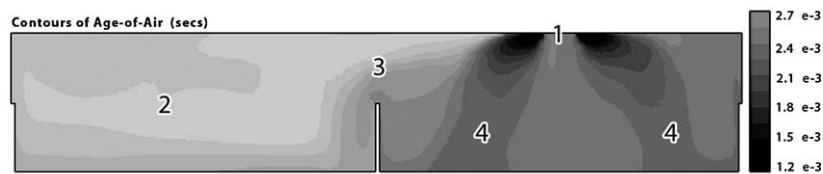


Fig. 8. Representative concentration gradients for two open zones, with right zone occupied and left zone unoccupied.

and are practical to be used for large open offices. Fig. 6b shows the difference between the average room temperatures in the occupied zone and the variable/unoccupied zone under the eight different scenarios. While the temperature values vary with the load scenarios, there is a consistent and distinct difference between the two zones when HVAC operation is turned off for the variable occupancy zone (Scenarios A-3, A-4, B-3, and B-4). This result suggests that the localized airflow provides a thermal containment effect, again demonstrated graphically in Fig. 5.

Airflow stability disturbance, such as side flow caused by opening to a staircase, is also important, as an unstable flow would invalidate the findings above. Fig. 7 shows the displacement of the throw from the diffuser from its target line with the introduction of a side flow. In an office building, a side flow could be generated from a pressure differential of an open door to a staircase or flow of a separate, dedicated ventilation system. For this study, up to a flow rate of 5 air exchange per hour (ACH), the side flow's effect on the shape of the localized flow is minimal (less than 10 cm). Only when the side flow approaches 15 ACH does significant deformation of the shape occur. This result indicates that the flow studied is very stable in normal operating conditions, and the previous airflow characteristics should hold true even when a side flow is present.

From the findings above, it is understood that the localized flow studied here is stable and attainable in an open office. The flow can also create a zoning effect in an open cubicle office. This nature of airflow isolation could also provide a unique opportunity for

indoor contaminant control, discussed in Section 3.3. Furthermore, while the airflow illustrated in Fig. 5 offers only a moderate thermal stratification, this phenomenon could provide considerable energy saving, discussed in Section 3.4.

3.3. Indoor air quality

The results from the age-of-air study described in Section 2.2 are shown in Fig. 8, with four areas of interest. Area 1 represents the surface average of the exhaust. Area 2 represents the volume average of the empty, unoccupied zone. Area 3 represents the plane boundary average between the two zones, and area 4 represents the occupied area inside the cubicles.

Taking volume and surface averaged age-of-air data in Fig. 8, the ventilation effectiveness values were calculated for area 1 through 4 and presented in Fig. 9. Specifically, data from area 1 (at the exhaust) represents the scenario where the two zones are well mixed. Finally, by refitting the CFD model using the formaldehyde source from carpet, cubicle walls and a point source, a new concentration model was derived and converted to contaminant removal effectiveness for each of the areas of concern, shown in Fig. 10.

The age-of-air gradient in Fig. 8 shows that a stagnation zone was created in the unoccupied zone (area 2 in Fig. 8). Data from Fig. 9a and b also indicate that there is no intensive air mixing between the occupied and unoccupied zones since areas 2 and 3 have significantly lower ventilation effectiveness. Also, the

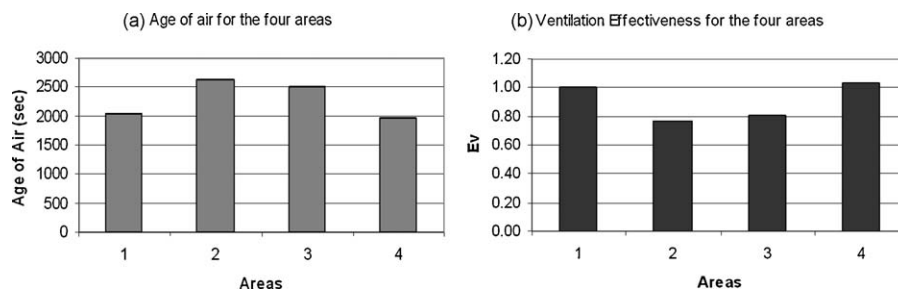


Fig. 9. Air mixing in the space (a) age of air and (b) ventilation effectiveness for the four areas presented in Fig. 8.

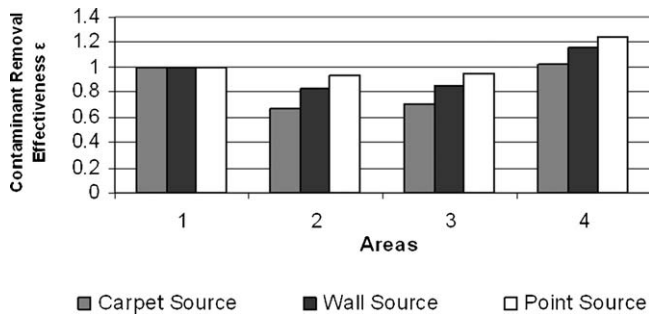


Fig. 10. Contaminant removal effectiveness for the three common types of pollution sources.

ventilation effectiveness of the occupied area 4 is higher compared to the well-mixed value (+2%), indicating a slight better ventilation performance. This finding suggests that the localized airflow is at least as good as delivering fresh air to occupants as well-mixed assumptions. The contaminant removal effectiveness for all three sources has similar patterns as the ventilation effectiveness (Figs. 9b and 10). These agreeing results show that with a localized air delivery system, pollutant concentrations in the occupied area (area 4) are lower than with the well-mixed air scenario. However, the stagnation zones (areas 2 and 3) have considerably higher contaminant concentrations resulting in lower contaminant removal effectiveness.

Additionally, the result for the contaminant confinement analysis for an emitting source in the cubicle is shown in Figs. 11 and 12, simulating a sick person surrounded by co-workers as a pollutant source. In Fig. 11, the CFD result visually displays the containment effect of the airflow, where the majority of the contaminant is confined within the emitting cubicle. This containment effect is further detailed in Fig. 12, where contaminant removal effectiveness is calculated for occupied areas in both zones.

The key difference between the results shown in Figs. 10 and 12 is that in Fig. 12, both zones are occupied in order to determine how the contaminant would spread in a scenario when the office space is full. From Fig. 11, it is clear the localized airflow contained the spread of contaminant inside the source zone, specifically when looking at the area between the two zones. Data shown in Fig. 12 further displays this phenomenon. Since the contaminant removal effectiveness of the “Far occupant area” is almost 2.5 times greater than the well-mixed scenario, it is obvious that the isolation effect of the airflow can prevent spread of contaminant, such as bacteria or virus from a sick office worker. One caveat is the performance of the near occupant area. By limiting the spread of the contaminant, the local concentration (near the source) is higher compared to the far occupant zone, with a contaminant removal effectiveness which is worse than in well-mixed scenario (Fig. 12). However, one can argue that in a scenario of disease control, stopping contaminant from spreading might have the higher priority than concerns of a high local pollutant concentration.

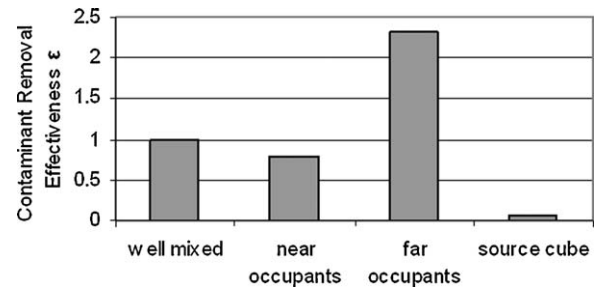


Fig. 12. Contaminant removal effectiveness for different areas (Fig. 11) in two adjacent occupied zones.

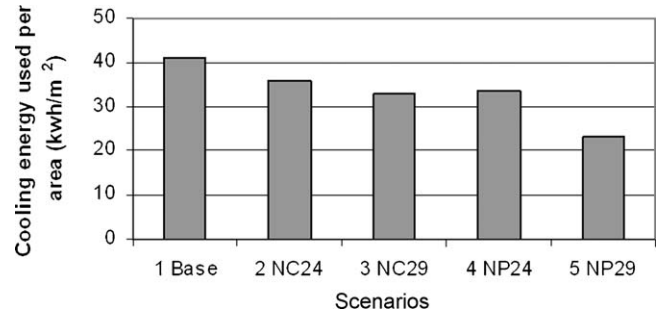


Fig. 13. Energy used for cooling in five scenarios described in Table 2 (NC = no core occupancy, NP = no perimeter occupancy; 24 and 29 = temperatures in the perimeter zone).

3.4. Energy simulations

As explained in Section 2.3, only the hottest three months were simulated to determine the effect of occupancy-based control on cooling energy consumption. It is important to point out that the conducted energy simulation is only a case study and is used to determine the potential energy saving, not to provide a realistic estimated saving in an office building.

Total cooling energy consumption is shown in Fig. 13, normalized by the area of the building. There are several findings based on comparison of the analyzed scenarios. By comparing scenario one (Base) to the other four, it is evident that occupancy-based HVAC control strategy could work, but the effectiveness varies based on different scenarios. Furthermore, comparison of scenarios two and three shows very little reduction in cooling energy consumption (6% reduction) when the core zone area (not adjacent to any exterior surfaces) is subjected to the occupancy control. However, comparison between scenarios four and five shows a different result. In scenario five, the building consumed significantly smaller amount of cooling energy (30% reduction) than in scenario four. Due to the identical setup of perimeter and core zones in scenarios four and five, this 30% energy saving can only come from the reduced conductive heat gains through the envelope caused by the higher temperature set point in the unoccupied perimeter zone.

Fig. 14 further confirms this finding with the result of the cooling loads of the perimeter zone when the temperature set

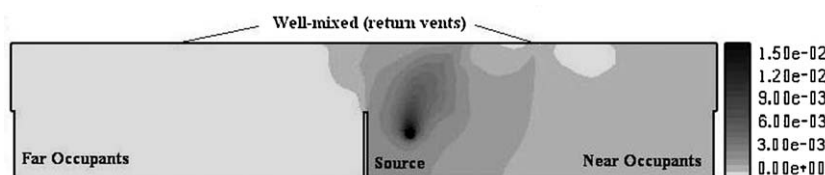


Fig. 11. Concentration gradients for two occupied zones with contaminant released in one of the cubicles.

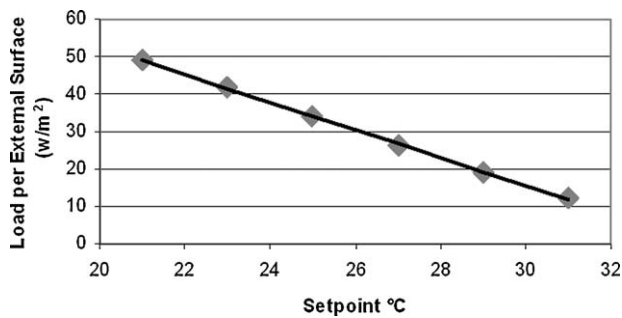


Fig. 14. Cooling load reduction as a function of perimeter zone temperature set point.

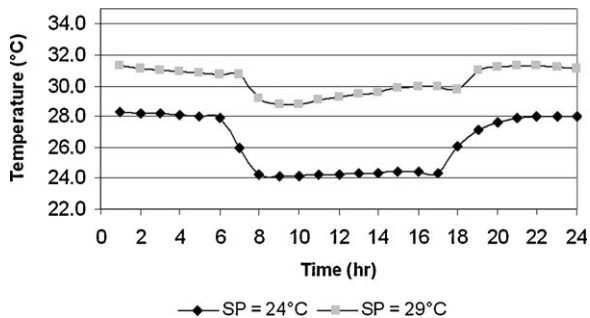


Fig. 15. Unoccupied perimeter zone temperatures during a typical cooling day with occupancy control (29 °C) and without (24 °C).

point is varied. It is evident that there is a direct relationship between the total cooling load in the perimeter zone and its temperature set point. This almost linear relationship suggests the majority of the cooling load in perimeter zone is coming from the external conduction heat gains.

While Fig. 13 shows the potential for significant energy saving when occupancy-based control strategy is used in perimeter zones, it is important to point out the energy saving dependency on the temperature in perimeter zones. The energy saving found comparing scenarios four and five is based on the temperature in perimeter zone increase from 24 to 29 °C, shown in Fig. 15.

However, this 5 °C temperature difference is more than 2 times of the 2 °C temperature difference found in the CFD study. This discrepancy significantly impacts the energy saving found in Fig. 13, and is further discussed in the following section.

4. General findings and study limitations

While results presented in previous section showed a possibly significant energy reduction in cooling scenarios, the calculated maximum saving of 30% is deceiving for all possible application due to the limitation of the energy model and climate zone. Without the ability to include a precise inter-zone airflow model, the DOE2 energy model simulated interaction between the zones as solid partitions. This causes the unoccupied perimeter zone temperature to rise to free floating temperature while keeping the occupied core zone at the set point, which is different than the CFD result. The energy simulation creates a larger averaged temperature difference (5 °C) compared to smaller difference (2 °C) found in the CFD airflow study. Luckily, the true cooling energy saving can still be estimated for the 2 °C scenario because of the almost linear relationship shown in Fig. 14. This linearity is due to the fact that vast majority of the energy saving is from the reduction of external conductive heat gain. At the temperature difference of 2 °C, the 30% saving (differences between occupancy scenarios four and five)

shown in Fig. 13 would reduce to approximately 12% saving of total cooling energy used, which is still a significant reduction. This shows that occupancy control can reduce cooling energy consumption when a significant temperature difference can be maintained between the occupied and the unoccupied areas, and when the external cooling load is prominent.

The benefit of localized airflow in terms of indoor air quality control is more straightforward. It is evident from Figs. 10 and 12 that the localized airflow has a distinct characteristic of removing general office pollutants as well as containing possibly bio-hazardous materials from spreading. If contaminant isolation and removal is important for a specific building, perhaps using localized airflow can be effective way to achieve such goal.

5. Conclusions

The validated CFD simulations showed that it is possible to produce a localized airflow in an open office space and to create relatively isolated zones. The two-zone analysis showed that the localized airflows in these zones are self-contained, but heat distribution makes the thermal isolation of this “open zone” less prominent. Temperature difference between occupied and unoccupied zones (zone with and without temperature control) of up to 2 °C indicates a potential for energy savings. The energy simulation results for the case study in Austin, TX found significant energy savings (approximately 12% of total cooling energy). However, the saving possibility should only be considered when the exterior cooling load through conduction is prominent, as well as when the temperature stratification in the perimeter zones of buildings is large.

Localized airflow also prevents large air mixing between occupied and unoccupied areas, thus creating relatively isolated and locally controlled environment. The ventilation effectiveness study showed that such environments can provide good indoor air quality. This finding addressed concerns related to degradation of indoor air quality by systems that does not provide high air mixing in a whole space. Furthermore, contaminant removal effectiveness results showed that occupancy-based air-conditioning can effectively remove contaminants from indoor sources, such as formaldehyde emitted from building furnishing materials. Finally, this specific airflow can be used to isolate contaminants (such as bio-hazardous materials, viruses and bacteria) within certain areas in a large open office space during an emergency situation.

Acknowledgement

This study is made possible by the National Science Foundation IGERT Program: grant #DGE-0549428, Indoor Environmental Science and Engineering—An Emerging Frontier.

References

- [1] Bureau of Labor Statistics, U.S. Department of Labor, Occupational Employment Statistics, May 2008. Available: <http://www.bls.gov/oes/> (accessed October 30, 2008).
- [2] P. Wargocki, D.P. Wyon, J. Sundell, G. Clausen, P.O. Fanger, The effects of outdoor air supply rate in an office on perceived air quality, Sick Building Syndrome (SBS) symptoms and productivity, *Indoor Air* 10 (4) (2000) 222–236.
- [3] W.J. Fisk, A.G. Mirer, M.J. Mendell, Quantitative relationship of sick building syndrome symptoms with ventilation rates, *Indoor Air* 19 (2) (2009) 159–165.
- [4] M.J. Mendell, A.G. Mirer, Indoor thermal factors and symptoms in office workers: findings from the US EPA BASE study, *Indoor Air* 19 (4) (2009) 291–302.
- [5] M. Fountain, G. Brager, E. Arens, Comfort control for short-term occupancy, *Energy and Buildings* 21 (1) (1994) 1–13.
- [6] A. Rabl, A. Rialhe, Energy signature models for commercial buildings—test with measured data and interpretation, *Energy and Buildings* 19 (2) (1992) 143–154.
- [7] Y. Huo, F. Haghghat, J.S. Zhang, C.Y. Shaw, A systematic approach to describe the air terminal device in CFD simulation for room air distribution analysis, *Building and Environment* 35 (2000) 563–576.

- [8] J. Srebric, Q. Chen, Simplified numerical models for complex air supply diffusers, *HVAC&R Research* 8 (3) (2002) 277–294.
- [9] V. Yakhot, S.A. Orszag, S. Thangam, Development of turbulence models for shear flows by a double expansion technique, *Physics of Fluids A* 4 (7) (1992) 1510–1520.
- [10] D. Rim, A. Novoselac, Transient simulation of airflow and pollutant dispersion under mixing flow and buoyancy driven flow regimes in residential buildings, *ASHRAE Transactions* 114 (2) (2008) 130–142.
- [11] A. Novoselac, J. Siegel, Impact of placement of portable air cleaning devices in multi-zone residential environment, *Building and Environment* 44 (12) (2009) 2348–2356.
- [12] ASHRAE, ASHRAE Standard 55, American Society of Heating Refrigeration and Air-conditioning Engineers, 2004.
- [13] D. Rim, A. Novoselac, Transport of particulate and gaseous pollutants in the vicinity of a human body, *Building and Environment* 44 (9) (2009) 1840–1849.
- [14] M. Sandberg, What is ventilation efficiency, *Building and Environment* 16 (2) (1981) 123–135.
- [15] C. Yu, D. Crump, A review of the emission of VOCs from polymeric materials used in buildings, *Building and Environment* 33 (6) (1998) 357–374.
- [16] D. Etheridge, M. Sandberg, *Building Ventilation: Theory and Measurement*, Wiley, New York, 1996.
- [17] S. Murakami, S. Kato, S. Nagano, Y. Tanaka, Diffusion characteristics of airborne particles with gravitational settling in a convection-dominant indoor flow field, *ASHRAE Transactions* 98 (1992) 82–97.
- [18] DOE-2.2, Lawrence Berkley Laboratory, Berkeley, CA, 2009. Available: <http://www.doe2.com> (accessed December 20, 2009).